animals

MDPI

Article

Automatic Recognition and Quantification Feeding Behaviors of Nursery Pigs Using Improved YOLOV5 and Feeding Functional Area Proposals

Yizhi Luo [1,2], Jinjin Xia [3], Huazhong Lu [2], Haowen Luo [1,2], Enli Lv [2,3], Zhixiong Zeng [3], Bin Li [2], Fanming Meng [2,4] and Aqing Yang [5,*]

[1] Institute of Facility Agriculture, Guangdong Academy of Agricultural Sciences, Guangzhou 510640, China; luoyizhi@gdaas.cn (Y.L.); wenyluyo@21cn.com (H.L.)
[2] State Key Laboratory of Swine and Poultry Breeding Industry, Guangzhou 510645, China; huazlu@scau.edu.cn (H.L.); enlilv@scau.edu.cn (E.L.); ganli180@sina.com (B.L.); mengfanming@gdaas.cn (F.M.)
[3] College of Engineering, South China Agricultural University, Guangzhou 510642, China; 2011010005@gdmec.edu.cn (J.X.); zhixzeng@scau.edu.cn (Z.Z.)
[4] Institute of Animal Science, Guangdong Academy of Agricultural Sciences, Guangzhou 510645, China
[5] College of Computer Science, Guangdong Polytechnic Normal University, Guangzhou 510665, China
* Correspondence: yangaqing1204@163.com; Tel.: +86-38308203

Simple Summary: In commercial-intensive pig farms, the identification and quantification of piglet feeding behavior is an important indicator for daily inspections. However, the model often judges pigs resting in the feeding area as the feeding behavior. Considering the functional characteristics of the pig house feeding area, we present a novel method based on the improved YOLOV5 and feeding functional area suggestions to identify the feeding and non-feeding behaviors of nursery piglets. In addition, four advanced models and ablation experiments are adopted for a comparative evaluation of the robustness of the model. This article proposes a model that can help the management team adjust piglet feeding patterns and save more manpower and feed.

Abstract: A novel method is proposed based on the improved YOLOV5 and feeding functional area proposals to identify the feeding behaviors of nursery piglets in a complex light and different posture environment. The method consists of three steps: first, the corner coordinates of the feeding functional area were set up by using the shape characteristics of the trough proposals and the ratio of the corner point to the image width and height to separate the irregular feeding area; second, a transformer module model was introduced based on YOLOV5 for highly accurate head detection; and third, the feeding behavior was recognized and counted by calculating the proportion of the head in the located feeding area. The pig head dataset was constructed, including 5040 training sets with 54,670 piglet head boxes, and 1200 test sets, and 25,330 piglet head boxes. The improved model achieves a 5.8% increase in the mAP and a 4.7% increase in the F1 score compared with the YOLOV5s model. The model is also applied to analyze the feeding pattern of group-housed nursery pigs in 24 h continuous monitoring and finds that nursing pigs have different feeding rhythms for the day and night, with peak feeding periods at 7:00–9:00 and 15:00–17:00 and decreased feeding periods at 12:00–14:00 and 0:00–6:00. The model provides a solution for identifying and quantifying pig feeding behaviors and offers a data basis for adjusting the farm feeding scheme.

Keywords: nursery pigs; feeding behavior recognition; functional area proposals; behavioral quantification; transformer

Citation: Luo, Y.; Xia, J.; Lu, H.; Luo, H.; Lv, E.; Zeng, Z.; Li, B.; Meng, F.; Yang, A. Automatic Recognition and Quantification Feeding Behaviors of Nursery Pigs Using Improved YOLOV5 and Feeding Functional Area Proposals. *Animals* **2024**, *14*, 569. https://doi.org/10.3390/ani14040569

Academic Editor: Daoliang Li

Received: 8 December 2023
Revised: 5 February 2024
Accepted: 5 February 2024
Published: 8 February 2024

1. Introduction

Automating the recognition and quantification of feeding behaviors in group-housed pigs can greatly assist in the identification of potential health and welfare issues [1–3].

A divergence in the food intake of pigs has been frequently linked to disease existence [4–6]. The continuous monitoring of pig feeding behavior will aid in the design of an appropriate feed delivery plan to help breeders regulate production plans, reduce the waste of fodder, and embrace the production potential of pigs [7–13]. However, individual pigs foraging or resting in the feeding area are often judged by the model as NFB (no feeding behavior) without consuming any feed [14]. The key to solving this problem is understanding how to distinguish the behavioral differences between feeding behavior and non-feeding behavior. Considering the functional characteristics of the pig house feeding area, the accurate identification of pig heads in the feeding area is a prerequisite for the identification of feeding behavior [15,16].

Several researchers have previously investigated systems for monitoring pig feeding behavior [17–20]. The methods are mainly based on wearable sensors (e.g., accelerometers, magnetometers, etc.) and non-contact video monitoring. As for contact electronic sensors, for instance, an electronic feeding system based on radio frequency identification (RFID) technology can monitor the meal interval per day of sows to assess their health status by assessing an individual pig's frequency of visits to feeders and water sources [13,21]. Kapun et al. proposed a feeding behavior recognition system for fattening pigs based on ultrahigh frequency (UHF-RFID) technology, which automatically reads the corresponding identity information when pigs are close to the feeding area or drinking area. The sensitivity of the system for feeding behavior and drinking behavior is 80% and 60%, respectively [13]. The above method used contact sensing radio frequency technology to identify the feeding and drinking behavior of pigs, but it is limited by the large labor cost required to install systems and tags and it remains somewhat invasive for pigs. Video monitoring is a low-cost, easy-to-maintain, and non-destructive monitoring technique. Zhu et al. identified individual pigs by calculating the Euclid distance between the pig and the standard sample and used it to determine whether the pig had drinking behavior based on the contact time between the pig and the drinking teat [22]. This method utilizes artificially designed features and is not accurate in other complex scenes. With the improvements in computing power, behavior recognition based on deep learning technology is widely used in the field of agriculture.

Compared with artificial features, the model based on deep learning can automatically learn the target features and improve the performance of the behavior recognition system [23–26]. A deep learning method with fully convolutional image processing was introduced to improve accuracy, which extracts the roundness of the head and the occlusion area between the head and the feeding area as spatial features based on the fully convolutional network (FCN), and it uses an optical flow vector to define the motion intensity of the head as a temporal feature, further improving the detection accuracy of the model [17]. However, current models such as Faster RCNN, YOLO, and CenterNet use a large number of proposals, anchors, or window centers, which are often less accurate in dense scenes. The transformer utilizes a self-attention mechanism for prediction, which performs well in the task of dense scene object detection. In addition, 3D cameras and thermal imaging cameras are also used in the field of animal behavior recognition [27–33].

In this work, we develop a single-view video analysis method to identify individual pigs and the numbers that engage in feeding behavior in large-scale pig herds without the need for additional sensors or individual markers. This approach differs from previous research in that it combines the location characteristics of the feeding area and the location of the pig head area where the feeding behavior occurs. In addition, a transformer module model was introduced based on YOLOV5 for pig head detection.

2. Materials and Methods

2.1. Animals, Housing, and Management

The experimental data in this paper were obtained from large-scale pig farms in Yunnan Province, China, from August to November 2021. The nursery barn of the pig farm consists of 28 pens with left and right symmetry (17 on one side), each 3.5 m long

and 2.2 m wide see Figure 1a below. The front doors and partitions of the pens are made of PVC sheets, the floor of each pen is all plastic, and it is equipped with one pen of five feeders and two drinking fountains see Figure 1c–e below. Each unit is equipped with an environmental control device and ventilation system to regulate the indoor temperature and humidity see Figure 1f–j below. The lighting time in the house is generally from 8:00 to 12:00 in the morning and from 14:00 to 18:00 in the afternoon.

In addition, there are a total of 2404 nursery pigs in the nursery barn, and the piglets in each nursery barn are all crossbred pigs and the starting weight is about 6.2 kg. The average activity area of each piglet is 0.35 square meters, in which they can obtain sufficient water and feed. The feeding method of the traditional mechanical trough is to put more than the theoretically required feeding amount into the trough according to the age of the pig and put it twice a day at 8:00 and 15:00. The indoor air data logging method is to record the room temperature, and the average relative humidity is set to every 5 min through the PR-3003WS-X USB temperature (PRSENS, Jinan, China) and humidity integrated data recorder produced by the PRSENS merchant (PRSENS, Jinan, China). The average room temperature is about 26.6 °C, and the average relative humidity is about 67.7%. The RGB camera (BA12-H, BA, Guangzhou, China) is used to collect data, which is connected to the server through a wireless network video recorder (WNVR), and the video is recorded and stored on the hard disk at the same time see Figure 1b below.

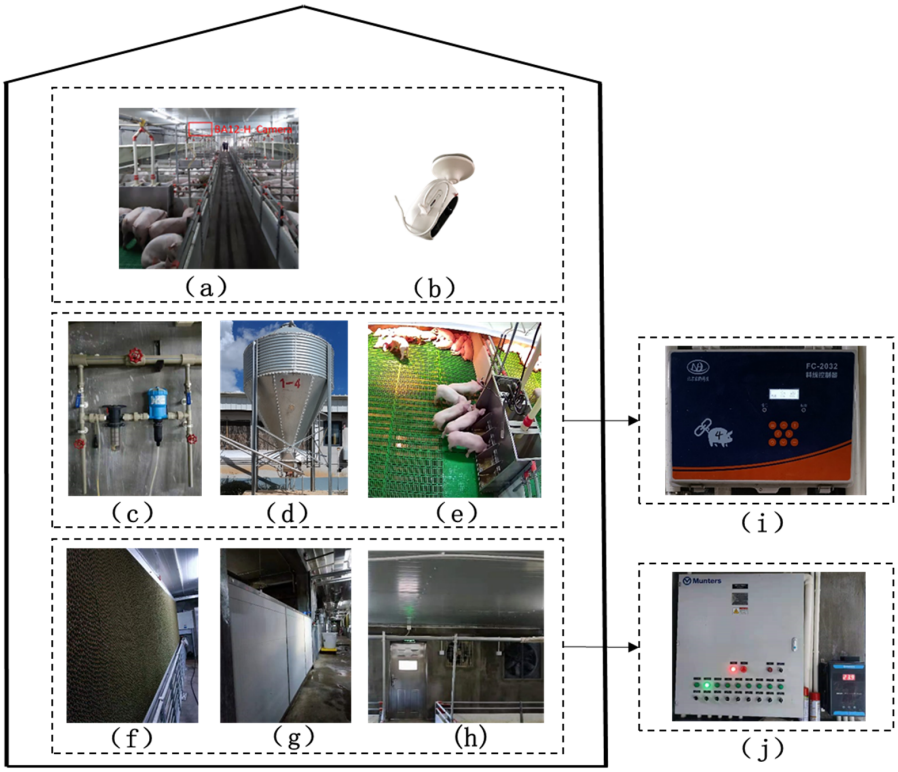

Figure 1. Description of the barn. (**a**) Inside the barn. (**b**) Camera placement area. (**c**) Water and drug mixing pipeline. (**d**) Feed supply. (**e**) Top view of pig pen. (**f**) Cooling wet curtain. (**g**) Air baffle. (**h**) Variable speed fan. (**i**) Environmental control controller. (**j**) Equipment master controller.

2.2. Dataset

2.2.1. Definition of Behaviors

Generally, the pig pen can be divided into five areas. As shown in Figure 2a, the red box ① is the drinking area, the yellow box ② is the feeding area, the orange box ③ is the resting area, and the purple box ④ and white box ⑤ are the areas for excretion and being active, respectively.

Based on data from the animal ethology literature [34], the definitions of feeding behavior and non-feeding behavior are shown in Table 1, and examples of the two behaviors are shown in Figure 2b,c. In particular, compared to the feeding behavior, the spatial position of the NFB is disturbing. As shown in Figure 2b, the head of the pig (No. 7) does not enter the trough, but near the trough the head behavior is considered NFB.

Table 1. Definition of pig behaviors.

Category	Abbreviation	Description
Feeding Behavior	FB	The piglet's head enters the trough, the head droops, and the two forelimbs enter or are near the trough.
Not Feeding Behavior	NFB	The piglet does not enter the trough, its head is not in the trough, its body is close to or away from the trough, and it stands on the floor vertically on all four limbs or lies on its side to rest.

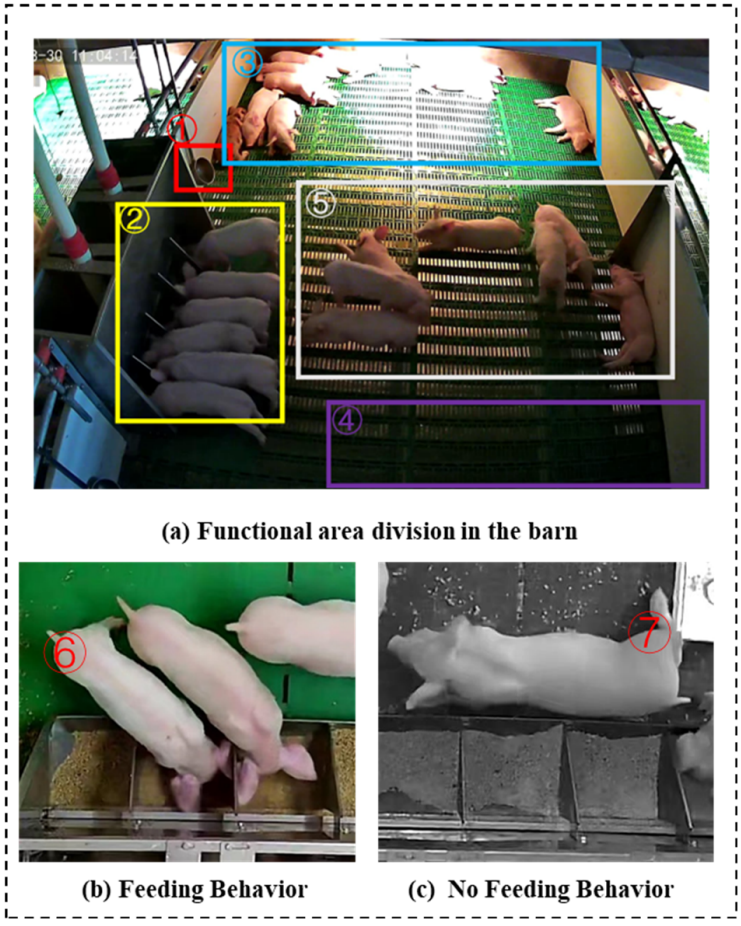

Figure 2. Schematic diagram of functional area distribution and behavior. (**a**) ① The drinking area, ② the feeding area, ③ the resting area, ④ the excretory area, and ⑤ the active area.

2.2.2. Data Acquisition and Preprocessing

Considering the application scenario characteristics of the model, 356 videos with differences in the skin color, light intensity, and posture of piglets were screened from all the data of a nursery barn. After video cutting pictures and data amplification, the final piglet head dataset is expanded to 6240, and the piglet head frame is about 80 K, including 5040 training sets and verification sets, with 54,670 piglet head boxes, 1200 test sets, and

25,330 piglet head boxes (Figure 3). The final data processing link is to use the interactive labeling tool Labelme (https://github.com/xwwwb/lableme_demo, accessed on 1 October 2021) to label the piglet head image, refer to the COCO dataset type, and export the .json file.

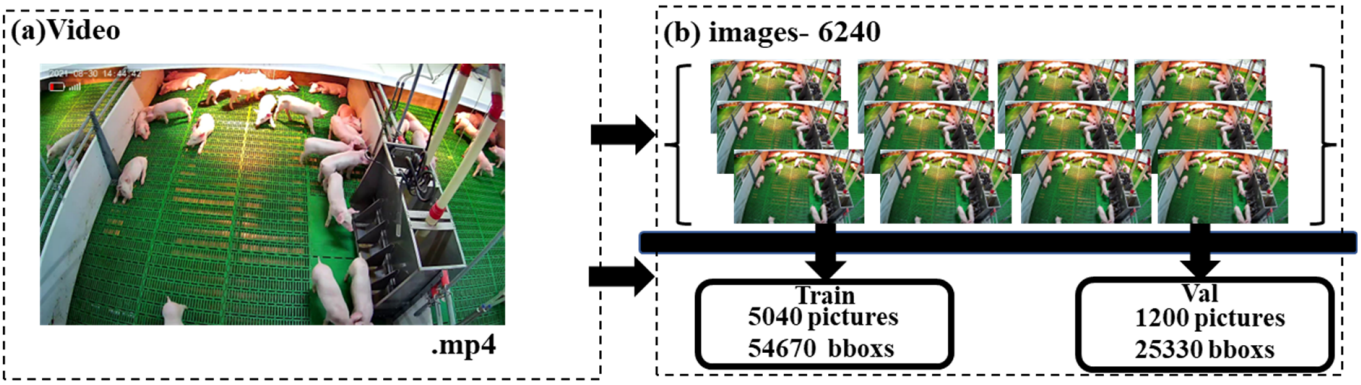

Figure 3. The constitution of our dataset.

2.3. The Overall Process of Behavior Recognition and Quantification

According to the behavior description of the pig feeding process in Table 1, during the feeding process the head of a piglet will enter the trough, and the body will remain stationary (without interference from other piglets) until the end of the feeding process. Therefore, in combination with the division of the functional areas inside the pigsty, a novel method is introduced based on deep learning and functional area proposals; the overall process is seen in Figure 4.

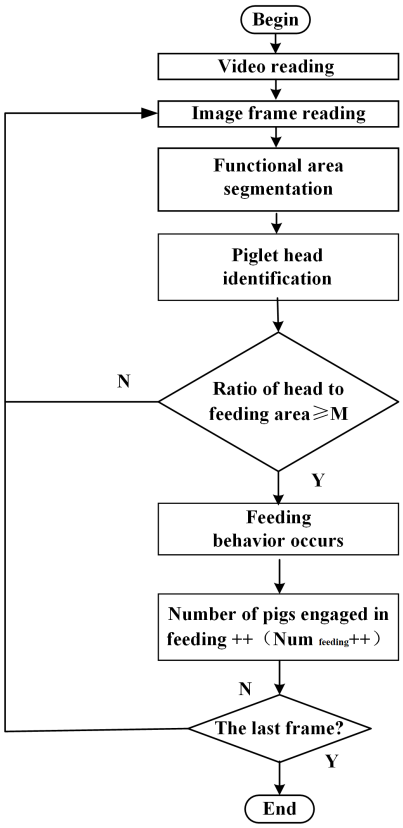

Figure 4. The overall process.

Feeding Functional Area Proposals Filtering Strategy

A traditional closed-loop area separation method is adopted in this paper to extract the feeding functional area proposals in the image (Algorithm 1). First, four coordinate points, L1, L2, R1, and R2, are selected according to the shape characteristics of the feed trough to represent the feeding area in the image. The location of the feeding area is shown in Figure 5a. Secondly, the closed feeding area A and the non-feeding area B are separated by setting the ratio of the coordinate points to the width and height of the image, as shown in Figure 5b. Finally, behavioral identification and quantity statistics are performed based on whether the piglet's head is in the feeding area and the number of piglets.

Algorithm 1 Feeding functional area proposals filtering strategy

input: Pig head detection bounding box $B[1...n]$
output: The number of feeding and drinking in the current frame $Num_{feeding}$

$Num_{feeding} \leftarrow 0; n \leftarrow 1$
for $i = 1 : Len(\mathrm{B[n]})$ **do**
  if B_1 $Area[Feeding]$ **then**
    $Num_{feeding} \leftarrow Num_{feeding} + 1$
  end if
end for
return $Num_{feeding}$

where $B[1...n]$ means all the bounding boxes are in the pig pen area, $Num_{feeding}$ means the number of heads with feeding behavior, and $Area[Feeding]$ means the extent of the feeding area.

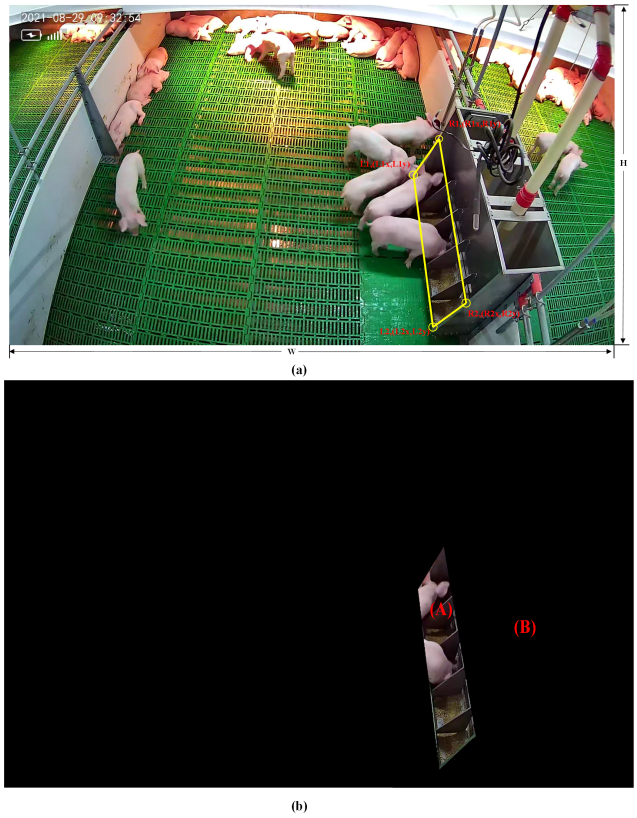

Figure 5. Example of feeding area location: (**a**) trough corner selection and (**b**) region of interest that may be feeding area.

2.4. Piglet Head Detection Network Architecture

Aiming to address the problems of piglet head occlusion, complex light in detecting feeding behavior, this paper proposes an improved deep learning model based on tph-YOLOV5 to realize piglet head detection in the region of interest for further characterizing the feeding behavior of piglets. Compared with the YOLOV4 model, YOLOV5 adopts the method of sharing convolution kernels to reduce the number of calculations, and reduce the number of model parameters, and improve the efficiency of network computing. The improved model architecture is shown in Figure 6, which is mainly composed of three parts, including the backbone feature extraction network, the neck network, and the prediction head.

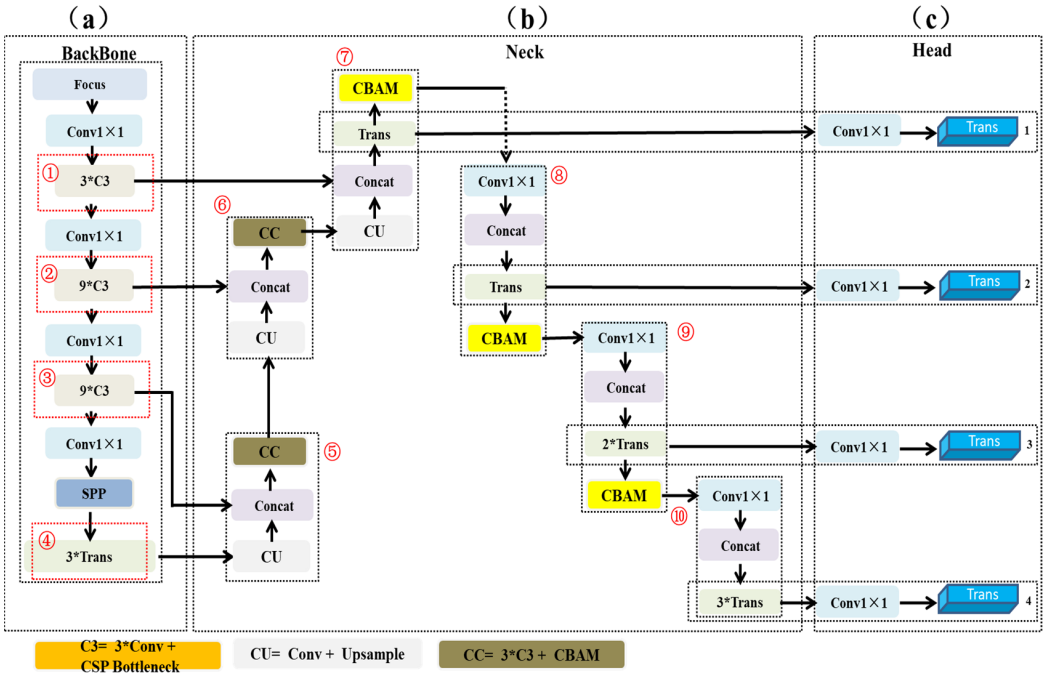

Figure 6. Piglet head detection network architecture: (**a**) the backbone of the model (**b**) the neck of the model and (**c**) the head of the model.

This study follows the main framework of tph-YOLOV5, as shown in Figure 6. First, the main structure adopts the C3 block (light gray block), which iterates 3, 9, and 9, respectively, as shown in Figure 6 ①, ②, and ③. Subsequently, a transformer module is added at the end of the backbone network to improve the ability to capture the features of the pig's head, as shown in Figure 6 ④ (light green block). On the one hand, this module enhances the ability of local information features of video frames [35]; on the other hand, it makes full use of context information to improve the feature extraction ability of the piglets' heads.

In the feature fusion part, a path aggregation network [36] is used to optimize feature reuse. Specially, upsampling is performed three times, respectively (Figure 6 ⑤, ⑥, and ⑦), and the convolutional block attention module (CBAM) is integrated into YOLOv5, which helps the model to find areas of interest in large-scale images (yellow block, Figure 6 ⑦, ⑧, and ⑨).

For the prediction head, different scales of feature maps are obtained by the operation of four 1 × 1 convolutions, as shown in Figure 6c. The pig is a non-rigid animal, and its head rotation, occlusion, distance from the camera, and other factors will affect the size of the piglets in the image. Therefore, the transformer module is added at the end of the prediction header. Moreover, the number of prediction headers is increased from three to four.

YOLO Principle

In practice, there are two types of target detection models: the two-stage model and one-stage model. Among them, Faster RCNN is a two-stage model that is used more in current research. The model introduces a region generation network (Region Proposal Network, RPN). Compared with RCNN, this model extracts the features of the input image and generates candidate regions at the same time to avoid duplication. Different from the Faster RCNN model, the YOLO series treats object detection as a regression problem and directly derives the piglet head position, category, and confidence level of the piglet head detection [37]. The structure is shown in Figure 7.

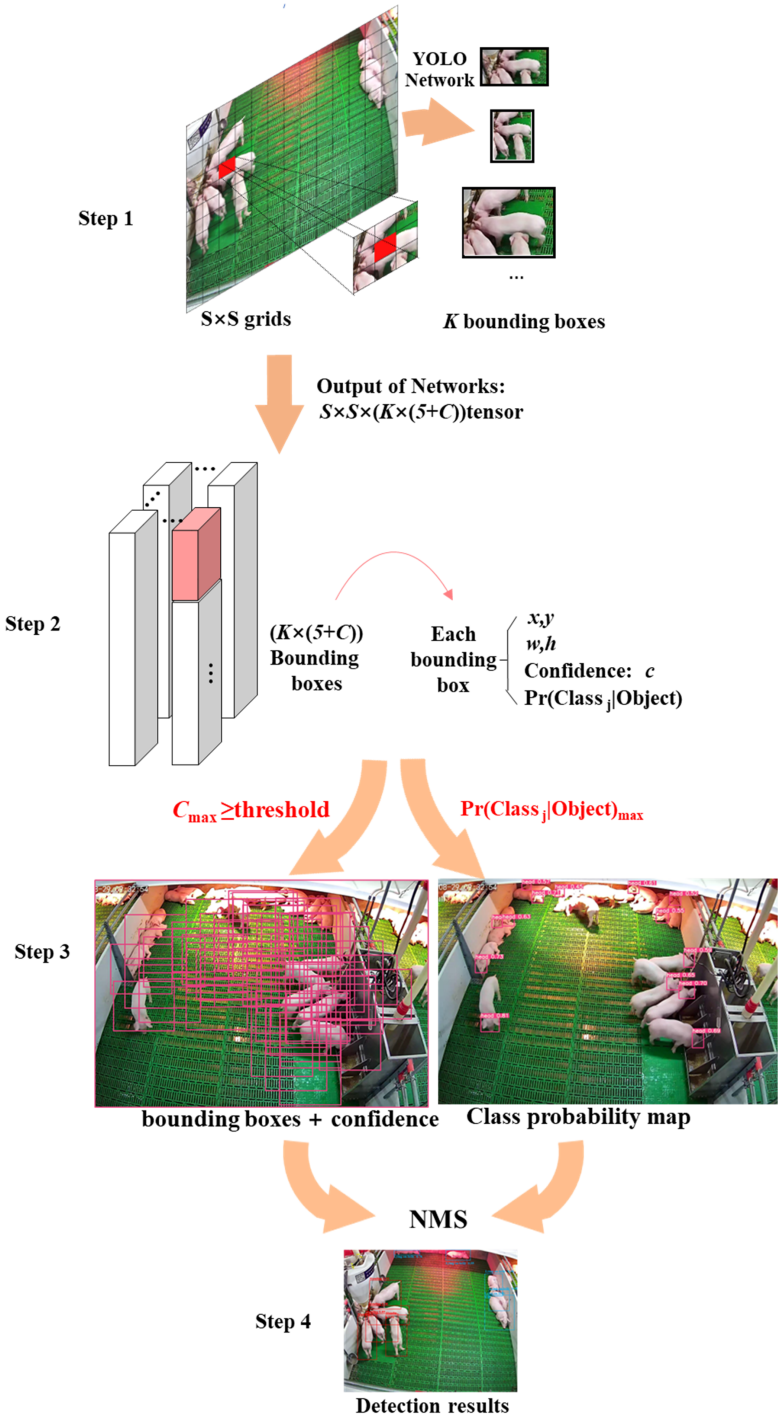

Figure 7. The primary principle of YOLO.

Initially, an image is divided into S × S grids, K bounding boxes are generated for each grid-based anchor box, and C represents the posture category of the pig; each bounding box contains six predicted values: x, y, w, h, confidence, and category probability (Pr). Among them, x, y, w, and h are used to describe the position of the bounding boxes, where the confidence represents whether the predicted box contains the object and the accuracy of the prediction box, and the pig posture category probability map is simultaneously generated. As stated in Formula (1), the confidence is the product of Pr and IOU. If the ground truth falls into this grid cell, Pr_{object} takes a value of 1; otherwise, it is 0. IOU is the intersection ratio between the bounding box and the actual ground truth, and the model employs non-maximum suppression to search for inhibiting redundant boxes.

$$Pr(Class_i|Objection_i) \times Pr(Object) \times IOU_{pred}^{truth} = Pr(Class_i) \times IOU_{pred}^{truth} \quad (1)$$

where Pr_{object} is $\in \{0, 1\}$.

The Intersection over Union (IOU) loss function is used for boundary box prediction to reflect the detection effect of the piglet head. As shown in Figure 8, the green box represents the real box and its area a, the blue box represents the prediction box and its area b, I is the intersection of the green box area and the blue box area, U is the union of the green box area and the blue box area, and $Loss_{iou}$ is the loss function, as shown in Formulas (2) and (3).

$$IOU = \frac{I}{U} \quad (2)$$

$$Loss_{iou} = -\ln(IOU) \quad (3)$$

where $\tilde{x} = (\tilde{x_t}, \tilde{x_b}, \tilde{x_l}, \tilde{x_r})$ represent the distances between the current pixel location (i, j) and the top, bottom, left, and right bounds of the ground truth, respectively. For simplicity, we omit footnote i, j in the rest of this paper. Accordingly, a predicted bounding box is defined as $x = (x_t, x_b, x_l, x_r)$.

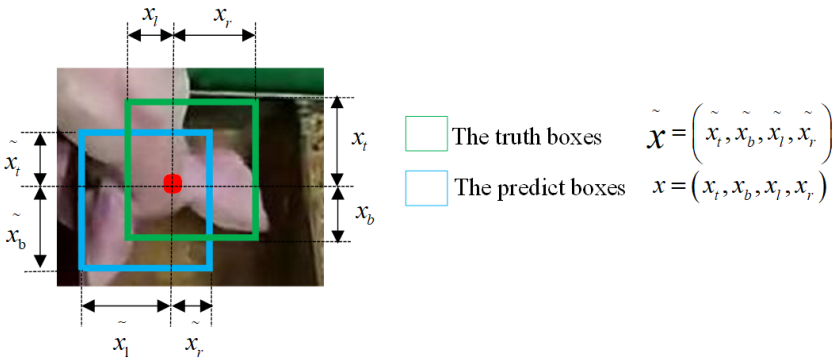

Figure 8. Schematic diagram of IOU prediction box loss.

The occlusion area, center point distance, and aspect ratio relationship between the predicted frame and the actual frame is taken into account in the CIOU loss function based on the DIOU; the formulas are shown in (4)–(6), and the schematic diagram of the CIOU computing structure is shown in Figure 9.

$$Loss_{ciou} = 1 - IOU + \frac{\rho^2(b, b^{gt})}{C^2} \quad (4)$$

$$\alpha = \frac{v}{(1 - IOU) + v} \quad (5)$$

$$v = \frac{4}{\pi^2}(\arctan\frac{w^{gt}}{h^{gt}} - \arctan\frac{w}{h})^2 \quad (6)$$

where b and b^{gt} represent the center points of the prediction box and the real box, respectively, and ρ represents the calculation of the Euclidean distance between the two center points, and C represents the diagonal distance of the minimum closure area that can contain both the prediction box and the true box, α is the parameter of the trade-off, and v is the parameter that measures the consistency of the aspect ratio.

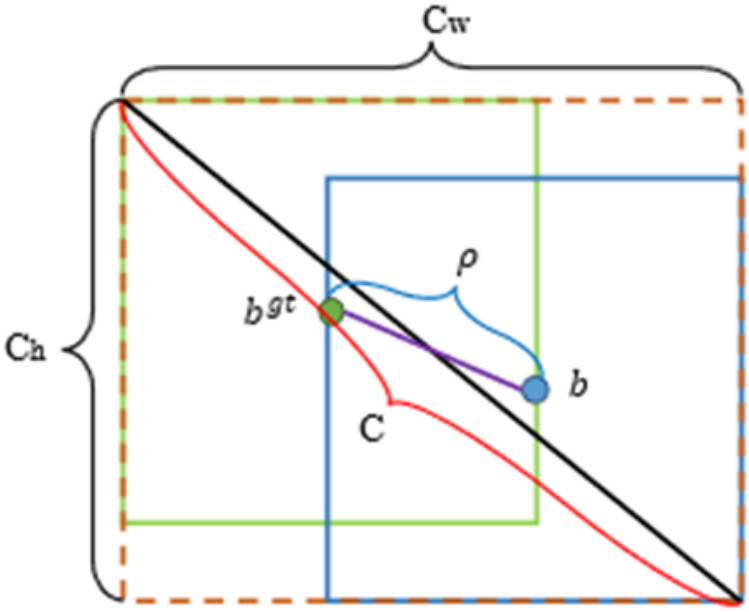

Figure 9. Schematic diagram of CIOU computing structure.

2.5. Evaluation Index

The mean average precision (mAP) and the F1 score (F1_score) are adopted to evaluate the effect of the pig head detection model in this paper [38]. The formulas for the mAP and the F1_score are as follows:

$$Precision = \frac{TP}{TP + FP} \tag{7}$$

$$Recall = \frac{TP}{TP + FN} \tag{8}$$

$$AP = \int_0^1 Precision \times Recalldr \tag{9}$$

$$mAP = \frac{AP}{n} \tag{10}$$

$$F1 - score = \frac{2(Precision \times Recall)}{Precision + Recall} \tag{11}$$

where n represents the classes, $n = 1$.

2.6. Training Environment and Equipment Description

In this paper, we adopt the Pytorch framework (https://pytorch.org/, accessed on 1 October 2021). The training environment and equipment description are shown in Table 2.

The initialization weights play an important roll in the process of network training. The hyperparameter optimization method is used in YOLOV5 [39], which uses a genetic algorithm for better model performance [40]. In this study, we use pretrained imageNet hyperparameters to fine-tune the pig head dataset.

Table 2. Training environment and equipment description.

Configuration	Parameter
Image resolution	2304 pixels ∗ 1296 pixels (W ∗ H)
Training framework	Python 3.7 programming language, Pytorch framework
Pretrained model	ImageNet model
Operating system	Ubuntu18.04 version
Accelerated environment	CUDA11 and CUDNN 7
Development environment	Vscode
Computer configuration used in training and testing	Dell Tower Workstation Intel@Xeon(R) T7920 Processor, 32 GB RDIMM, 512 G Solid State Drive, 4 TB Mechanical Hard Drive, Graphics Card RTX2080Ti

3. Results

3.1. Performance Comparison of Different Models

Video analysis is one of the main daily tasks of managers. A novel feeding behavior recognition and quantification model was proposed in this paper to help administrators extract effective information from a large scale of similar videos for the timely detection of abnormalities in pig herds. Simultaneously, four advanced models were adopted for a comparative evaluation on the pig head dataset, including YOLOV3 (DarkNet53), YOLOV5 (CSPDarknet53), YOLOV5 (MobileNetV3-Large), and YOLOV5 (RepVGG), as detailed in Table 3. Compared with the yolov5 model, the model in this article improved the mAP index and F1_score index by 5.8% and 4.7%, respectively.

Table 3. Performance comparison of different models.

Detector	Backbone	mAP	F1_Score
YoloV3	Darknet53	83.1%	82.0%
YoloV5	CSPDarknet53	87.0%	86.0%
YoloV5	MobileNetV3-Large	66.4%	66.0%
YoloV5	RepVGG	78.0%	77.0%
YoloV5	proposed model	92.1%	90%

In addition, we analyzed the confidence loss (Figure 10a) and bounding box loss (Figure 10b) after 300 epochs. The loss function is one of the main indicators for model performance evaluation. It can be seen that with the increase in the number of training epochs, the loss values of both models show a steady downward trend, and the curves are smoother. The reason for the rapid decline in the category loss was attributed to a single category (piglet head).

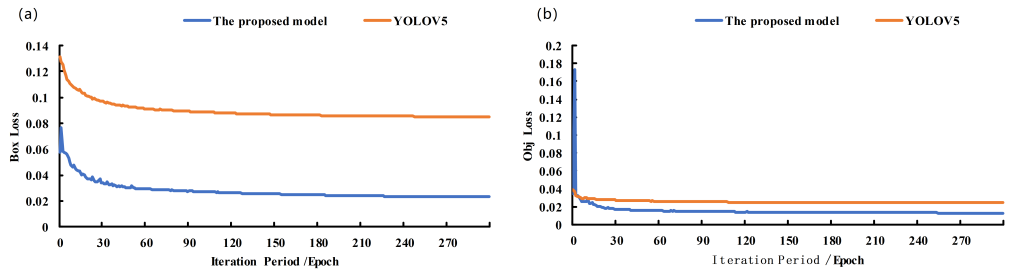

Figure 10. Train loss for the YOLOV5+Transform (the proposed model) and YOLOV5. (**a**) Box loss. (**b**) Obj loss.

In particular, the two models were basically stable in the first 120 epochs, and the loss of the proposed model dropped faster and lower. In addition, the mAP0.5, the precision rate, and the recall rate were evaluated, and they are reported in Figure 11. The results show that the evaluation indicators of the proposed model are better than for YOLOV5.

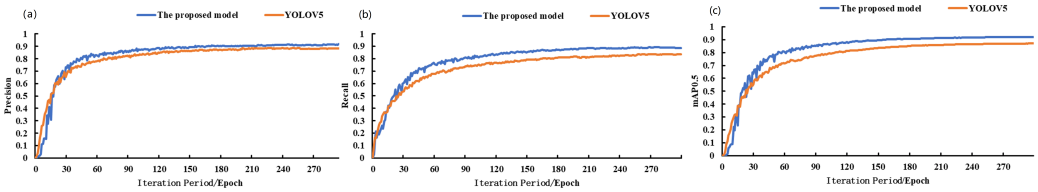

Figure 11. Train loss for the proposed model and YOLOV5. (**a**) Precision. (**b**) Recall. (**c**) mAP0.5.

3.2. Ablation Test

In order to evaluate the effectiveness of each improvement to the model proposed in this paper, ablation experiments were conducted to analyze the causal relationship of each improved component. The experiment was divided into five groups, namely, M0–M4. The test results are shown in Table 4.

Table 4. Ablation test.

Classes	C3TR	CBAM	Change Head	mAP	F1_Score
M0	-	-	-	87.0%	86.0%
M1	✓	-	-	89.4%	87.0%
M2	-	✓	-	87.2%	86.0%
M3	-	-	✓	87.4%	85.0%
M4	✓	✓	✓	92.1%	90%

M0 = YOLOv5s, M1 = YOLOv5s + C3TR, M2 = YOLOv5s + CBAM, M3 = YOLOv5s + changed head, and M4 = YOLOv5s + C3TR + CBAM + changed head.

3.3. Performance Comparison of Three IOU Loss Functions

Moreover, three IOU loss functions were used for the comparative analysis in this paper, including Generalized IOU (GIOU loss), Distance IOU loss (DIOU), and Complete IOU loss (CIOU). The results are shown in Table 5. The CIOU loss function performed best in the model performance matrix, with the mAP and F1 being 0.921 and 0.90, respectively. In the regression of the boundary box, the coupling characteristics between the size of the piglet head boundary and its position were better coordinated.

Table 5. Model performance results for different IOUs.

Model	IOU	mAP	F1_Score
The proposed model	GIOU	87.2%	87%
The proposed model	DIOU	89.4%%	87%
The proposed model	CIOU	92.1%%	90%

4. Discussions

4.1. The Impact of Different Models on the Pig Head Detection Performance

A representative sample is selected in this work to compare the performances of different models in recognizing pig heads. Figure 12b (orange elliptical area, left) shows a complex lighting scene (heat preservation lamp). An interesting phenomenon is that no false detections occurred under the occlusion of the pig's head and forelimbs (black area in Figure 12b). This also reflects the powerful ability of deep learning in feature extraction. Figure 12c (purple elliptical area, right) shows the situation of the occlusion scene. The comparison results show that some lightweight models (e.g. MobileNetV3-Large) perform poorly in obstructed mountains, and their ability to extract features from pig heads is not strong. In addition,target occlusion of the same category is a specific challenge in agricultural target detection applications. Missed detection will occur due to the non-maximum suppression (NMS) operation to remove redundant frames, also representing a future research direction.

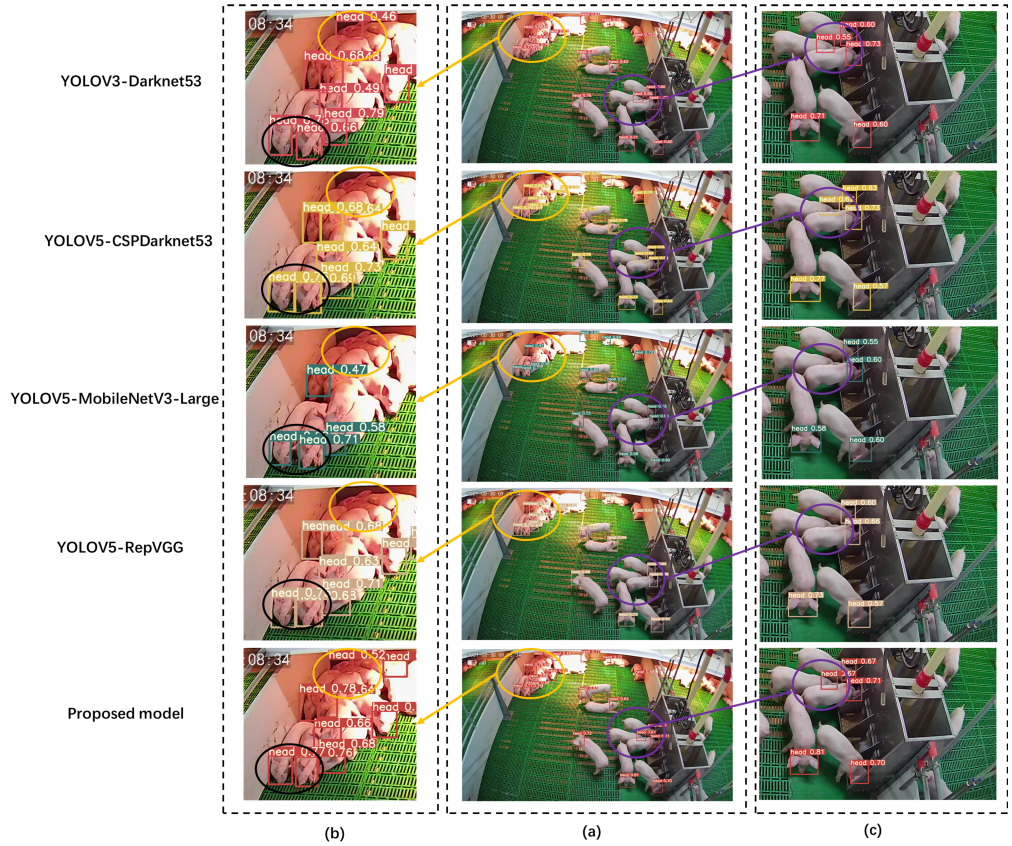

Figure 12. Detection effects of different models. (**a**) Example. (**b**) Partial enlargement 1 of the example. (**c**) Partial enlargement 2 of the example.

4.2. Results of Feeding Behaviors and No Feeding Behaviors

We randomly selected 24 continuous hours of video data and saved the test results in a .txt file containing the identification results of the feeding behavior and no feeding behavior and their corresponding quantities.

Figure 13 shows examples of head detection in FB and NFB recognition and the corresponding heatmap [41]. The Grad CAM method was introduced to use the gradient of the object class relative to the feature map to visualize the class differentiation and location in the input image. As shown in Figure 13b,d, the red areas in the heatmap represent the regions of interest in the model. The pigs' heads were activated in the heatmap, reflecting the pig head detection ability of the model.

A previous study extracted spatiotemporal features from videos to recognize the feed behaviors of nursery pigs and further improved the recognition accuracy by changing the video length and frame rate [19]. In contrast to the task of video classification, this paper focused on the detection of pig feeding behavior at the image frame level, which can be used to quantify the herd behavior of pigs and reflect their health status.

As shown in Figure 13c, the pig is considered as having NFB even though there are piglets near the trough. In addition, compared to the detection of the heating lamp area (complex lighting conditions), the result performance is better in the feeding area. Lighting conditions have always been a huge challenge for image processing. One study used a 3D camera to handle sow pose detection under complex lighting conditions, with significant advantages in resisting lighting and spatial coordinate relationships. Compared with RGB cameras, 3D cameras have smaller viewing angles and are more expensive.

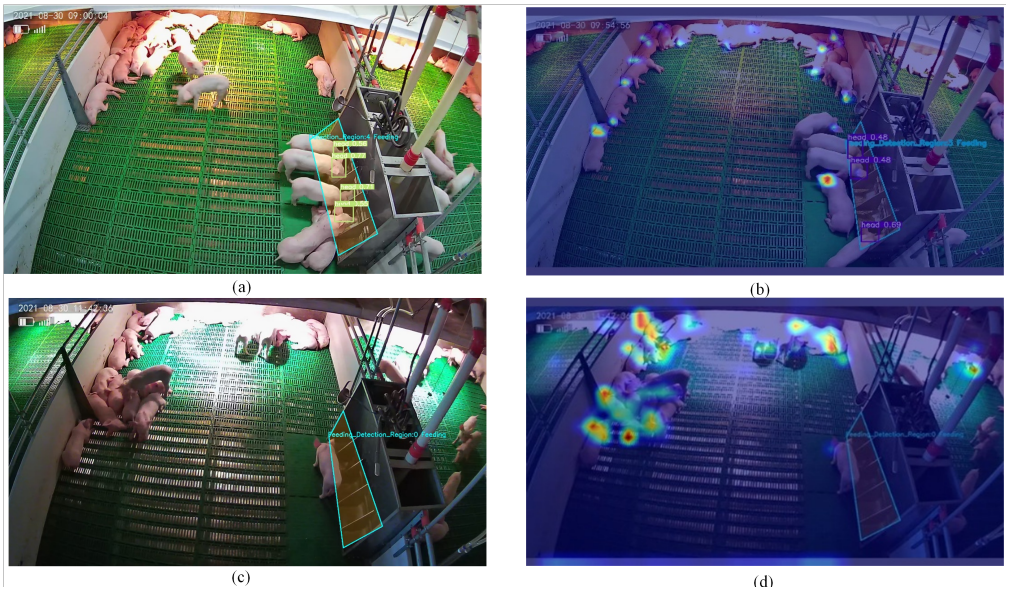

Figure 13. Behavior quantification examples and category heatmap visualization. (**a**) Feeding behavior. (**b**) Heatmap visualization of feeding behavior. (**c**) Not feeding behavior. (**d**) Heatmap visualization of no feeding behavior.

Distribution of Feeding Time of Piglets in Different Periods for All Weather

Figure 14 shows the distribution of the feeding and drinking time of the piglets across different all-weather periods. From the total consumption trends of feeding and drinking, the piglets ate and drank at the same time. The total consumption time of food and water for the piglets demonstrated a similar change trend, including the three feeding peaks (5:00–6:00 GMT, 15:00–17:00 GMT, and 20:00–21:00 GMT). The feeding behavior of the pigs increased in the period from 7:00 to 8:00 GMT, when most of the piglets woke up. From 10:00 to 11:00 GMT, their feeding behavior decreased slightly. Before the noon break, their feeding behavior increased. After 12:00 GMT, the keepers turned off the fluorescent lamp, and the piglets began to rest. Their feeding behavior gradually decreased. From 14:00 to 15:00 GMT, a large number of piglets woke up to feed, and, until 18:00 GMT, the fluorescent lamp was turned off. The last peak appeared at night when the keepers were patrolling. Therefore, the feeding behavior of the piglets demonstrated clear day and night characteristics, with intermittent feeding, and was affected by the feeding environment.

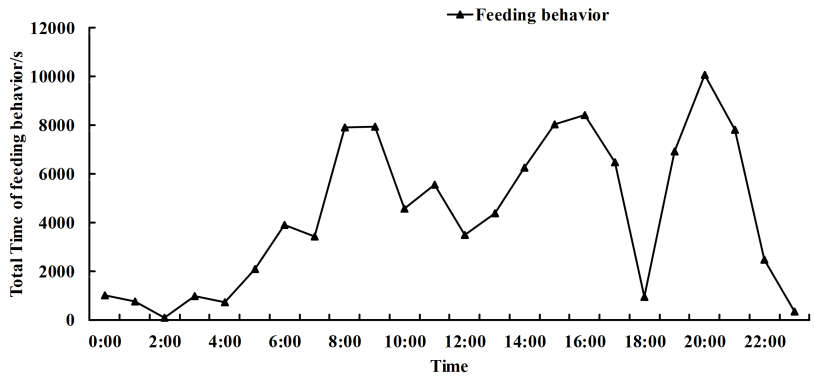

Figure 14. Feeding time of all piglets in different periods (all weather).

In addition, there was a statistical distribution of the maximum number of piglets in the all-weather feeding periods. As shown in Figure 15, the peak and trough of the feeding appeared alternately, indicating that the food intake of the pigs was phased. The red line

represents the feeder space. It can be seen from the trend of the curve in the figure that the number of piglets feeding was larger than that of the feeder space in the periods from 5:00 to 12:00 GMT, 15:00 to 16:00 GMT, and 20:00 to 21:00 GMT, and it exceeded it by 50% in the periods from 7:00 to 9:00 GMT and 20:00 to 21:00 GMT. In addition, the number of piglets feeding was lower than the feeder space at 22:00–5:00 GMT. During this period, only a few piglets fed intermittently, as the feeding peak often occurred before and after the pigs slept; this provides a reference for breeders when developing feeding plans.

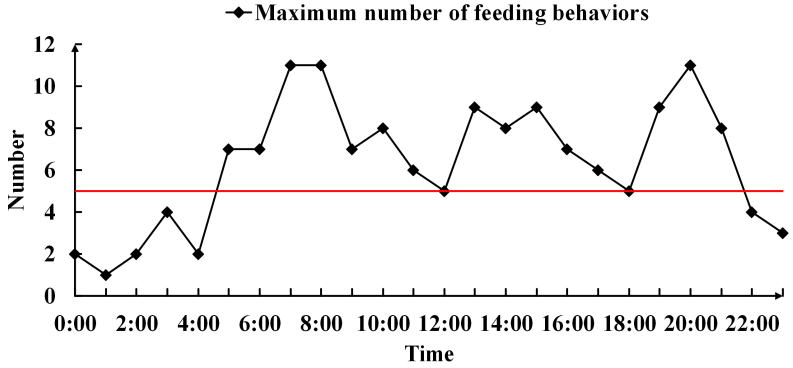

Figure 15. (Maximum number of piglets feeding behavior (all-weather).

5. Conclusions

Continuous automated monitoring of pig feeding behavior can help breeders standardize production plans, reduce feed waste, and give full play to pig production potential. However, manual inspection statistics are a heavy workload and highly subjective, which is not conducive to production needs. This work proposes a new method based on the improved yolov5 and feeding functional area suggestions to identify feeding and non-feeding behaviors of nursery piglets, simplifying complex feeding behaviors into a functional area piglet head detection problem. Particularly, in piglet head detection, compared with YOLOV5, the improved model achieved a mAP increase of 5.8% and an F1_score increase of 4.7%. At the same time, the model was applied to the analysis of the feeding patterns of nursery pigs raised in groups for 24 h of continuous monitoring. It was found that the feeding rhythms of nursery pigs are different in the day and night. The peak feeding period is 7:00–9:00 and 15:00–17:00. And the feeding time is from 12:00 to 14:00 and 0:00 to 6:00. This model provides a solution for identifying and quantifying pig feeding behavior and provides a solution for adjusting pig farm feeding programs that provide the basis for the data. In addition, according to the effect of model detection, objects of the same category will be missed in detection due to the NMS operation to remove redundant frames, which is also a future research direction.

Author Contributions: Conceptualization, Y.L., A.Y. and J.X.; methodology, J.X., H.L. (Huazhong Lu) and H.L. (Haowen Luo); software, E.L. and Z.Z.; validation, F.M., Y.L. and J.X.; formal analysis, J.X., B.L. and A.Y.; investigation, H.L. (Haowen Luo) and H.L. (Huazhong Lu); resources, E.L., Z.Z. and H.L. (Haowen Luo); data curation, Y.L. and H.L. (Haowen Luo); writing—original draft preparation, Y.L., A.Y. and H.L. (Huazhong Lu); writing—review and editing, A.Y. and Y.L.; visualization, F.M., E.L. and H.L. (Huazhong Lu); funding acquisition, H.L. (Haowen Luo), A.Y. and B.L. All authors have read and agreed to the published version of the manuscript.

Funding: This research was funded by the Fundamental Research Funds for the State Key Laboratory of Swine and Poultry Breeding Industry (ZQQZ-25), (2023QZ-NK16), National Natural Science Foundation of China (32202733); Guangzhou Science and Technology Planning Project (2023A04J0127); Project of Educational Commission of Guangdong Province of China (2021KQNCX044); and the Project of Collaborative Innovation Center of GDAAS-XTXM202201 (Research on environmental regulation and optimization of planting and breeding facilities in South China (XT202203)).

Institutional Review Board Statement: Not applicable for studies not involving humans or animals

Informed Consent Statement: Informed consent was obtained from all subjects involved in the study

Data Availability Statement: Data are contained within the article.

Acknowledgments: We acknowledge the Yunnan DBN Agricultural Commercial Pig Farm for the use of their animals and facilities. We also thank Ultralytics for developing the YOLOV5 architecture (https://github.com/ultralytics/yolov5, accessed on 1 September 2021), from which the code was extended for this project, and the Pytorch framework (https://pytorch.org/, accessed on 1 October 2021) adopted to train the deep learning models.

Conflicts of Interest: The authors declare no conflicts of interest.

References

1. Nguyen-Ba, H.; van Milgen, J.; Taghipoor, M. A procedure to quantify the feed intake response of growing pigs to perturbations. *Animal* **2020**, *14*, 253–260. [CrossRef]
2. Neethirajan, S.; Reimert, I.; Kemp, B. Measuring Farm Animal Emotions—Sensor-Based Approaches. *Sensors* **2021**, *21*, 553. [CrossRef]
3. Jia, M.; Zhang, H.; Xu, J.; Su, Y.; Zhu, W. Feeding frequency affects the growth performance, nutrient digestion and absorption of growing pigs with the same daily feed intake. *Livest. Sci.* **2021**, *250*, 104558. [CrossRef]
4. Von Jasmund, N.; Wellnitz, A.; Krommweh, M.S.; Büscher, W. Using Passive Infrared Detectors to Record Group Activity and Activity in Certain Focus Areas in Fattening Pigs. *Animals* **2020**, *10*, 792. [CrossRef]
5. Boumans, I.J.; de Boer, I.J.; Hofstede, G.J.; Bokkers, E.A. How social factors and behavioural strategies affect feeding and social interaction patterns in pigs. *Physiol. Behav.* **2018**, *194*, 23–40. [CrossRef]
6. Li, Y.; Zhang, H.; Johnston, L.; Martin, W. Understanding Tail-Biting in Pigs through Social Network Analysis. *Animals* **2018**, *8*, 13. [CrossRef]
7. Li, Y.Z.; Johnston, L.J.; Dawkins, M.S. Utilization of Optical Flow Algorithms to Monitor Development of Tail Biting Outbreaks in Pigs. *Animals* **2020**, *10*, 323. [CrossRef] [PubMed]
8. Vitali, M.; Santolini, E.; Bovo, M.; Tassinari, P.; Torreggiani, D.; Trevisi, P. Behavior and Welfare of Undocked Heavy Pigs Raised in Buildings with Different Ventilation Systems. *Animals* **2021**, *11*, 2338. [CrossRef] [PubMed]
9. Luo, Y.; Zeng, Z.; Lu, H.; Lv, E. Posture Detection of Individual Pigs Based on Lightweight Convolution Neural Networks and Efficient Channel-Wise Attention. *Sensors* **2021**, *21*, 8369. [CrossRef] [PubMed]
10. Juul, L.; Kristensen, T.; Theil, P.; Therkildsen, M.; Kongsted, A. Effect of two different feeding strategies on energy intake from pasture, feed efficiency and growth performance of growing-finishing pigs in a mobile pasture system. *Livest. Sci.* **2021**, *252*, 104690. [CrossRef]
11. Gomes, B.C.K.; Andretta, I.; Valk, M.; Pomar, C.; Hauschild, L.; Fraga, A.Z.; Kipper, M.; Trevizan, L.; Remus, A. Prandial Correlations and Structure of the Ingestive Behavior of Pigs in Precision Feeding Programs. *Animals* **2021**, *11*, 2998. [CrossRef]
12. Larsen, M.L.V.; Wang, M.; Norton, T. Information Technologies for Welfare Monitoring in Pigs and Their Relation to Welfare Quality®. *Sustainability* **2021**, *13*, 692. [CrossRef]
13. Kapun, A.; Adrion, F.; Gallmann, E. Case Study on Recording Pigs' Daily Activity Patterns with a UHF-RFID System. *Agriculture* **2020**, *10*, 542. [CrossRef]
14. Alameer, A.; Kyriazakis, I.; Dalton, H.A.; Miller, A.L.; Bacardit, J. Automatic recognition of feeding and foraging behaviour in pigs using deep learning. *Biosyst. Eng.* **2020**, *197*, 91–104. [CrossRef]
15. Ott, S.; Moons, C.; Kashiha, M.; Bahr, C.; Tuyttens, F.; Berckmans, D.; Niewold, T. Automated video analysis of pig activity at pen level highly correlates to human observations of behavioural activities. *Livest. Sci.* **2014**, *160*, 132–137. [CrossRef]
16. Arulmozhi, E.; Bhujel, A.; Moon, B.E.; Kim, H.T. The Application of Cameras in Precision Pig Farming: An Overview for Swine-Keeping Professionals. *Animals* **2021**, *11*, 2343. [CrossRef] [PubMed]
17. Yang, A.; Huang, H.; Zheng, B.; Li, S.; Gan, H.; Chen, C.; Yang, X.; Xue, Y. An automatic recognition framework for sow daily behaviours based on motion and image analyses. *Biosyst. Eng.* **2020**, *192*, 56–71. [CrossRef]
18. Li, Y.Z.; McDonald, K.A.; Gonyou, H.W. Determining feeder space allowance across feed forms and water availability in the feeder for growing-finishing pigs. *J. Swine Health Prod.* **2017**, *25*, 9. [CrossRef] [PubMed]
19. Chen, C.; Zhu, W.; Steibel, J.; Siegford, J.; Han, J.; Norton, T. Classification of drinking and drinker-playing in pigs by a video-based deep learning method. *Biosyst. Eng.* **2020**, *196*, 1–14. [CrossRef]
20. Chen, C.; Zhu, W.; Steibel, J.; Siegford, J.; Han, J.; Norton, T. Recognition of feeding behaviour of pigs and determination of feeding time of each pig by a video-based deep learning method. *Comput. Electron. Agric.* **2020**, *176*, 105642. [CrossRef]
21. Garrido-Izard, M.; Correa, E.C.; Requejo, J.M.; Diezma, B. Continuous Monitoring of Pigs in Fattening Using a Multi-Sensor System: Behavior Patterns. *Animals* **2019**, *10*, 52. [CrossRef]
22. Zhu, W.; Guo, Y.; Jiao, P.; Ma, C..; Chen, C. Recognition and drinking behaviour analysis of individual pigs based on machine vision. *Livest. Sci.* **2017**, *205*, 129–136. [CrossRef]

23. Kim, M.; Choi, Y.; Lee, J.; Sa, S.; Cho, H. A deep learning-based approach for feeding behavior recognition of weanling pigs. *J. Anim. Sci. Technol.* **2021**, *63*, 1453–1463. [CrossRef]
24. Parez, S.; Dilshad, N.; Alanazi, T.M.; Lee, J.W. Towards Sustainable Agricultural Systems: A Lightweight Deep Learning Model for Plant Disease Detection. *Comput. Syst. Sci. Eng.* **2023**, *47*, 515–536. [CrossRef]
25. Dilshad, N. Efficient Deep Learning Framework for Fire Detection in Complex Surveillance Environment. *Comput. Syst. Sci. Eng.* **2023**, *46*, 749–764. [CrossRef]
26. Yar, H.; Khan, Z.A.; Ullah, F.U.M.; Ullah, W.; Baik, S.W. A modified YOLOv5 architecture for efficient fire detection in smart cities. *Expert Syst. Appl.* **2023**, *231*, 120465. [CrossRef]
27. Lou, M.E.; Porter, S.T.; Massey, J.S.; Ventura, B.; Deen, J.; Li, Y. The Application of 3D Landmark-Based Geometric Morphometrics towards Refinement of the Piglet Grimace Scale. *Animals* **2022**, *12*, 1944. [CrossRef]
28. Li, G.; Hui, X.; Chen, Z.; Chesser, G.D.; Zhao, Y. Development and evaluation of a method to detect broilers continuously walking around feeder as an indication of restricted feeding behaviors. *Comput. Electron. Agric.* **2021**, *181*, 105982. [CrossRef]
29. Del Valle, J.E.; Pereira, D.F.; Mollo Neto, M.; Gabriel Filho, L.R.A.; Salgado, D.D. Unrest index for estimating thermal comfort of poultry birds (Gallus gallus domesticus) using computer vision techniques. *Biosyst. Eng.* **2021**, *206*, 123–134. [CrossRef]
30. Gómez, Y.; Stygar, A.H.; Boumans, I.J.M.M.; Bokkers, E.A.M.; Pedersen, L.J.; Niemi, J.K.; Pastell, M.; Manteca, X.; Llonch, P. A Systematic Review on Validated Precision Livestock Farming Technologies for Pig Production and Its Potential to Assess Animal Welfare. *Front. Vet. Sci.* **2021**, *8*, 660565. [CrossRef] [PubMed]
31. Yang, Q.; Xiao, D.; Cai, J. Pig mounting behaviour recognition based on video spatial–temporal features. *Biosyst. Eng.* **2021**, *206*, 55–66. [CrossRef]
32. Li, X.; Pan, J.; Xie, F.; Zeng, J.; Li, Q.; Huang, X.; Liu, D.; Wang, X. Fast and accurate green pepper detection in complex backgrounds via an improved Yolov4-tiny model. *Comput. Electron. Agric.* **2021**, *191*, 106503. [CrossRef]
33. Gan, H.; Xu, C.; Hou, W.; Guo, J.; Liu, K.; Xue, Y. Spatiotemporal graph convolutional network for automated detection and analysis of social behaviours among pre-weaning piglets. *Biosyst. Eng.* **2022**, *217*, 102–114. [CrossRef]
34. Yang, Q.; Xiao, D. A review of video-based pig behavior recognition. *Appl. Anim. Behav. Sci.* **2020**, *233*, 105146. [CrossRef]
35. Xu, S.; Dutta, V.; He, X.; Matsumaru, T. A Transformer-Based Model for Super-resolution of Anime Image. *Sensors* **2022**, *22*, 8126. [CrossRef]
36. Liu, S.; Qi, L.; Qin, H.; Shi, J.; Jia, J. Path aggregation network for instance segmentation. In Proceedings of the IEEE Conference on Computer Vision and Pattern Recognition, Salt Lake City, UT, USA, 18–23 June 2018; pp. 8759–8768.
37. Zhu, X.; Lyu, S.; Wang, X.; Zhao, Q. TPH-YOLOv5: Improved YOLOv5 Based on Transformer Prediction Head for Object Detection on Drone-captured Scenarios. In Proceedings of the 2021 IEEE/CVF International Conference on Computer Vision Workshops (ICCVW), IEEE, Montreal, BC, Canada, 11–17 October 2021; pp. 2778–2788. [CrossRef]
38. Chen, C.; Zhu, W.; Norton, T. Behaviour recognition of pigs and cattle: Journey from computer vision to deep learning. *Comput. Electron. Agric.* **2021**, *187*, 106255. [CrossRef]
39. Mekhalfi, M.L.; Nicolò, C.; Bazi, Y.; Al Rahhal, M.M.; Alsharif, N.A.; Al Maghayreh, E. Contrasting YOLOv5, Transformer, and EfficientDet Detectors for Crop Circle Detection in Desert. *IEEE Geosci. Remote. Sens. Lett.* **2021**, *19*, 3003205. [CrossRef]
40. Han, J.H.; Choi, D.J.; Park, S.; Hong, S.K. Hyperparameter optimization using a genetic algorithm considering verification time in a convolutional neural network. *J. Electr. Eng. Technol.* **2020**, *15*, 721–726. [CrossRef]
41. Selvaraju, R.R.; Cogswell, M.; Das, A.; Vedantam, R.; Parikh, D.; Batra, D. Grad-CAM: Visual Explanations From Deep Networks via Gradient-Based Localization. In Proceedings of the IEEE International Conference on Computer Vision, Venice, Italy, 22–29 October 2017; p. 9.